Thesis for the degree
Master of Science

Submitted to the Scientific Council of the
Weizmann Institute of Science
Rehovot, Israel

עבודת גמר (תזה) לתואר
מוסמך למדעים

מוגשת למועצה המדעית של
מכון ויצמן למדע
רחובות, ישראל

By
Hagai Edri

מאת
חגי אדרי

התעבות בוז-איינשטיין במלכודת מגנטית עם פוטנציאל אופטי
Bose-Einstein Condensate in an Optically Plugged Magnetic Trap

Advisor:
Prof. Nir Davidson

מנחה:
פרופ' ניר דודזון

December, 2014

טבת, תשע"ה

Abstract

Cold atoms have been a exciting field of research in the last 35 years [1, 2], especially since the observation of Bose-Einstein Condensation (BEC) in 1995 [3, 4]. Many experiments have been done studying the properties of ultracold atoms. The ability to tune interaction strengths by Feshbach resonances [5, 6] and to apply external potentials with optical lattices [7], has created the opportunity of probing many-body physics using ultracold dilute gasses in a highly controlled manner.

In this thesis I report the observation and characterization of ^{87}Rb BEC in a quadrupole magnetic trap with a blue-detuned laser beam at the center of the trap (Optically Plugged Magnetic Trap)[8, 9]. When cold atoms are put in a magnetic field, their spin interacts with the field and a force is exerted on them. When that force is a restoring force the atoms can be trapped by the magnetic field. However, if the magnetic field vanishes at some point in space a non-adiabatic spin flip can occur, the force direction will change and the atoms will be removed from the trap. To avoid these Majorana losses [10] we use a high intensity blue-detuned laser beam that exerts a repulsive force on the atoms and prevents them from getting to the region with low magnetic field.

To cool the atoms to quantum degeneracy we use RF induced evaporative cooling [11]. In this method the RF field interacts only with the hottest atoms in the trap and transfers them to a different magnetic state where the magnetic force pushes the atoms from the trap. We have studied and characterized the trap, evaporation process and BEC.

We intend to use this trap to sympathetically cool ^{40}K atoms (fermions) with the ^{87}Rb to achieve degenerate Fermi gas of ^{40}K atoms to be used in our future experiments.

Acknowledgments

For the past year and a half I've had the opportunity to work with excellent people in a great atmosphere that helped me work on my project and find my way in the experimental physics world.

I would like to express my gratitude to my supervisor, Prof. Nir Davidson for many insightful conversations during the work on this project, for his guidance and patience and for giving me the opportunity to conduct my study in his research group.

I would also like to thank my lab partners Asif Sinai, Noam Matzliah and Dr. Alok Singh who joined us recently, for teaching me how to work in a lab, for the long discussions and friendly advices, and for making it a lot more fun. Furthermore I would like to thank the rest of the people in our group for their help and support: Jonathan Coslovsky, Gadi Afek, Slava Smartsev, Ronen Chriki, Chene Tradonsky, Dr. Vishwa Pal, David Egger, Dr. Rostyslav Baron and Alexander Mil .

A special thanks to Dr. Yehonatan Dallal and Ravid Shaniv for sharing their knowledge with me and offering their advice.

Finally, none of this would have been possible without the love and support of the people around me, my partner for life Ilana Rojkov and my close family.

Contents

1 Introduction

Experiments with ultracold atoms have become a fundamental tool in physics research. The first experimental realizations in 1995 of Bose-Einstein condensation (BEC) in dilute atomic gases [3, 4] marked the beginning of a very rapid development in this field. Ultracold dilute gas clouds provide a controlled and isolated environment to explore many-body physics phenomena. The atoms give rise to collective phenomena related to those observed in solids, quantum liquids, and nuclei.

Experimentally these systems are attractive to work with, since atoms can be manipulated by lasers and magnetic fields. In addition, the ability to image the atoms on a CCD camera allows a direct measurement of local properties of the cloud that are not easily accessible in other many-body systems. The possibility to control atomic interactions with a magnetic Feshbach resonances [6, 5] has been a very important achievement. It is a powerful tool in ultracold gases that allows experimentalists to challenge many-body theories and explore systems with long range correlations and strong interactions where theory is not available.

In recent years, after extensive research about bosonic atoms, ultra cold fermions have become an exciting research area. Fermionic superfluids have been observed close to a Feshbach resonance [12, 13], where the superfluid changes smoothly from BEC to BCS superfluid. The possibility to build model systems and control them to high precision has led to the notion that ultracold atoms can be used as quantum simulators, perhaps answering the question once presented by Feynman [14].

In this thesis I report on the formation of a Bose-Einstein condensation in a optically plugged magnetic trap. These measurements were done in the process of building an apparatus for exploring many-body physics with ultracold gasses of ^{87}Rb (bosons) and ^{40}K (fermions). My project was assembling the optical plug system (a focused $532nm$ laser beam that repels atoms from the center of the trap where Majorana loss is significant), building the RF system used for evaporative cooling and proving they can be used to achieve quantum degeneracy, which is clearly seen by the formation of a BEC.

The work on the apparatus was done cooperatively with Asif Sinai and Noam Matzliah. I chose to focus this thesis on the parts in the apparatus that were designed, assembled and operated by me, namely the Optical Plug and RF Evaporation systems.

1.1 Cold Atoms Experiments Overview

Every cold atom system has its own unique features, its advantages and weaknesses, but there are some steps that has to happen in order to get an ultracold atoms experiment going. The basic tools are optical scattering force and dipole force, and magnetic force due to interaction with the atoms spin.

The first step in the experimental sequence is cooling the atoms from the room temperature to the Doppler limit temperature or close to it, and trapping them. This is usually done by a

Magneto Optical Trap (MOT, see section 2.2.1) in a high vacuum chamber $\sim 10^{-8} torr$. The atoms can get to the chamber directly from a non evaporative getter, or by other methods [15].

After capturing the cooled atoms in a MOT, several other techniques are used to cool them beyond the Doppler limit and increase density. In our system we first compress the atoms by dark MOT [16] and immediately after that we use Polarization Gradient Cooling [17] (Sisyphus cooling, PGC). The goal of these steps is to get the highest phase space density before the evaporation process.

The next step is trapping the atoms without laser cooling and using evaporative cooling [11] to get to quantum degeneracy. This step is longer (several seconds or more) because the atoms need to collide and thermalize many times during evaporation, for this reason many cold atom experiments transport the atoms to a second vacuum chamber with higher vacuum where the atoms have longer lifetime in the trap and they are not lost in the evaporation process. There are several methods to transfer the atoms over a long distance [18, 19], we use magnetic transport (see section 2.2.2). If magnetic trapping is used then a stage of optical pumping to a specific magnetic state is done before trapping the atoms to increase trapping efficiency.

In our system we release atoms from the getters (getters are working continuously to achieve constant conditions in the chamber), we capture the atoms in the MOT, compress them and use PGC. After optical pumping we trap the atoms in a magnetic trap and transfer them over a 42 cm long, L shaped tube to our second chamber. There we trap the atoms in a strong optically plugged magnetic trap and use RF induced evaporative cooling. After 12 seconds of evaporation we get a BEC of about 10^5 atoms.

1.2 Majorana Losses in a Magnetic Trap

An atom with magnetic moment μ in a magnetic field B has an energy of $U_B = -\mu \cdot \mathbf{B}$, for an atom in a state $\left|F\ m_f\right\rangle$, where F is the total spin of the atom and m_f is magnetic quantum number, this corresponds to a Zeeman energy $U = \mu_B g_f m_f B$, where g_f is the Landé factor and μ_B is Bohr magneton. In a non-uniform field the force acting on the atoms in direction $\hat{n}$ will be $F_{\hat{n}} = -\mu_B g_f m_f \vec{\nabla} |B| \cdot \hat{n}$. For atoms in a state with $g_f m_f > 0$ (trappable state) this is a restoring force that confines the atoms close to the local magnetic field minimum, as the magnetic energy decreases as the atom moves into a lower field. However, if an atom is in a magnetic trap and its spin changes to an untrappable state (i.e. $g_f m_f < 0$) the magnetic force will change direction, and the potential will have the form of an anti-trap. The atom will be attracted to the magnetic field maximum and will be lost from the trap. This loss mechanism is referred to as Majorana spin flip [10].

The atom is trapped as long as its magnetic moment can follow the direction of the magnetic field adiabatically as it moves through the trap. If the change in the magnetic field occurs too fast, the atoms spin can flip non-adiabatically into an untrappable state. The 2 time scales involved are the atoms precession frequency around the magnetic field - Larmor frequency

$\omega_L = \frac{\mu_B |m_f g_f B|}{\hbar}$, and the change rate of the magnetic field $\left|\frac{\dot{B}}{B}\right|$ which can be estimated for an atom at velocity v moving over a distance r as $\left|\frac{\dot{B}}{B}\right| \approx \frac{v}{r}$. The adiabatic condition is $\omega_L \gg \left|\frac{\dot{B}}{B}\right|$, the atoms will be confined as long as it is fulfilled. For small magnetic fields this condition is hard to fulfill and the possibility of a non-adiabatic spin flip is significant.

In a magnetic quadrupole trap [20], the magnetic field vanishes at the center and atoms will be lost due to these Majorana spin flips in a region of an ellipsoid around the center (usually referred to as a hole). The flux of atoms through the ellipsoid will be the loss rate.

1.2.1 Estimating the Loss Rate

To estimate the loss rate in a magnetic quadrupole trap we approximate the ellipsoid as a sphere [21], the sphere radius is where the adiabatic condition breaks down.

$$\omega_L = \left|\frac{\dot{B}}{B}\right| = \frac{v}{r_{hole}} \Rightarrow r_{hole} \sim \left|\frac{v\hbar}{\mu_B m_f g_f \frac{dB}{dr}}\right|^{\frac{1}{2}} \tag{1}$$

The flux of atoms through the sphere is $\Gamma = \frac{N}{l^3} \cdot \pi r_{hole}^2 \cdot v$, with N the number of atoms in the trap, and l the cloud size. Using the virial theorem we can estimate the cloud size $mv^2 \sim \mu \frac{dB}{dr} l$, lastly we can relate the mean velocity of the atoms to the cloud temperature. Neglecting numerical constants on the order of 1, we get the loss rate:

$$\Gamma \simeq N \frac{\hbar}{m} \left(\frac{\mu_B m_f g_f \frac{dB}{dr}}{k_B T}\right)^2 \tag{2}$$

In our trap for ^{87}Rb with $\frac{dB}{dr} = 90\ \frac{G}{cm}$ in a temperature of $30\mu K$, $\frac{\Gamma}{N} \approx 0.3\ sec^{-1}$ and $r_{hole} \approx 1\mu m$.

This estimation shows that Majorana losses are most significant at low temperatures, when the atoms get closer to the center. In a magnetic quadrupole trap all atoms will be lost in the evaporation process if Majorana losses are not accounted for.

There are several methods to prevent Majorana losses, we chose to use a high intensity off-resonant laser directed to the center of the trap that creates a potential barrier and prevents the atoms from getting close to the hole [4, 8] (see section 2.3.2).

1.3 Evaporative Cooling

Laser cooling by the optical molasses technique and polarization gradients [17] produces atoms with a temperature below the Doppler limit, but considerably above the recoil limit. A very effective way to reduce the temperature of the atoms further is to evaporative cool [11] them after they have been confined in a magnetic trap. This process is similar to the way that a cup of tea loses heat as the steam carries energy away, the cloud of atoms in a magnetic trap cools when the hottest atoms are allowed to escape. Each atom that leaves the trap carries away more

than the average amount of energy and so the remaining gas gets colder. The remaining trapped, lower energy atoms rethermalize by elastic collisions and acquires a new, lower temperature.

The time it takes for the cloud to thermalize depends on the rate of collisions between atoms in the trap. An efficient evaporation is characterized by the fact that the elastic collision rate $\Gamma_{coll} =< n \cdot \sigma \cdot v >$ is large compared to the loss rate, where n is the cloud density, v is the atom velocity and σ denotes the s-wave scattering cross-section between the atoms. To have an efficient evaporation, the collision rate should increase in the process despite decreasing number of atoms, such "runaway evaporation" is reached when $\frac{d\log\Gamma}{dt} > 0$. Through evaporative cooling it is possible to reduce the temperature several orders of magnitude and increases the phase-space density to a value at which quantum statistics becomes important.

To have an efficient evaporation process we would like to have a selective method to take only the hottest atoms from the trap and remove them in a controlled manner, without changing the trap. Our primary method for evaporative cooling is inducing transition between trappable and untrappable states using radio frequency (RF) radiation, when an atom is radiated with RF frequency that correspond to the Zeeman splitting between 2 Zeeman states with $\Delta m_f = 1$ it can adiabatically transfer to a different magnetic state. If that state is untrappable then it will be removed from the trap.

Starting with high frequencies (compared to the cloud temperature) and reducing the RF frequency in the process we can remove only the hottest atoms at each step and the cloud gets colder. This method is selective because only high energy atoms reach the regions in the trap corresponding to high magnetic fields and high Zeeman splitting energy, thus only they are affected by the RF radiation. It allows us to keep the trap constant during the evaporation, and the process is easily controlled by the amplitude and frequency of the RF radiation. Another evaporation method is to have a sticky wall close to the clouds edge which absorbs most energetic atoms. In our apparatus the cloud is very close to the cell walls and some of the hot atoms are absorbed in the wall which causes some uncontrolled evaporation (see section 3.1).

In the case of fermions the situation is different. The requirement of the antisymmetry of the wave function (Pauli exclusion principle) causes the scattering cross section for fermions at the same internal state to vanish at low temperatures. Therefore evaporative cooling of fermions, with all atoms in the same internal state, cannot work. We can overcome this difficulty by using a mixture of fermions in different internal states from the same isotope, or a mixture of bosons and fermions. In a bosons-fermions mixture the bosons collide with themselves and with the fermions in the evaporation process and they cool the fermions by sympathetic cooling [22]. We use bosons and fermions mixture (^{87}Rb and ^{40}K), in a magnetic trap we can evaporate the ^{87}Rb atoms without evaporating the high energy ^{40}K atoms, so that the trapped ^{40}K will not be lost due to evaporation. This is possible because the Zeeman splitting for ^{87}Rb is larger than for ^{40}K in the same magnetic field, therefore they will interact with the RF field at higher frequencies and the ^{40}K will be cooled by sympathetic cooling and move to lower magnetic fields before it will interact with the RF field.

2 Experimental Setup

2.1 Overview of Apparatus

Our apparatus consists of 2 vacuum cells (a MOT cell and Science cell hereafter, commonly used in the ultracold atoms community) connected by an L shaped tube that enables differential pumping and UHV in the science cell ($< 10^{-11} torr$). The vacuum is generated by a 55 liter ion pump ,connected to the MOT cell and another 150 liter ion pump, connected close to the science cell. In the MOT cell we have 5 getters, 2 of Rb^{87} and 3 of K^{40}, these provide atoms for the experiment. They also release a lot of unwanted atoms to cell that causes high pressure ($10^{-8} torr$).

In the MOT cell we have built a double species Magneto Optical Trap (see section 2.2.1) that captures the atoms and cools them from room temperature to $\sim 300\mu K$, after compression of the cloud and further sub-Doppler cooling [17] we load the atoms to a magnetic trap. The magnetic trap potential is then moved over a $42cm$ L shaped tube to the science cell. That is done by running suitable currents through a chain of 15 coil pairs, thus changing the position of the magnetic trap without changing its geometry [19]. The atoms follow the trap adiabatically without significant heating of the cloud.

Our science cell is very small compared to other similar systems, it has a size of $8mm \times 8mm$ with wall thickness of $1.5mm$ (Starna). This allows us better optical access, a large numerical aperture in the imaging system and it is easier to get to UHV. On the other hand, it limits our time of flight imaging in the cell and affects the lifetime of large atomic clouds in the magnetic trap (see section 3.1). In the science cell we trap the atoms in an optically plugged magnetic trap, this trap is a combination of a linear magnetic potential and a repulsive optical potential of a blue-detuned Gaussian beam (see sections 2.3.1, 2.3.2). With RF induced evaporation we cool the atoms to sub micro Kelvin temperature and a Bose-Einstein condensate of ^{87}Rb is formed.

The apparatus was designed to transport ^{40}K atoms with the ^{87}Rb to the science cell to produce a degenerate Fermi gas of ^{40}K through sympathetic cooling, but this has not been achieved yet.

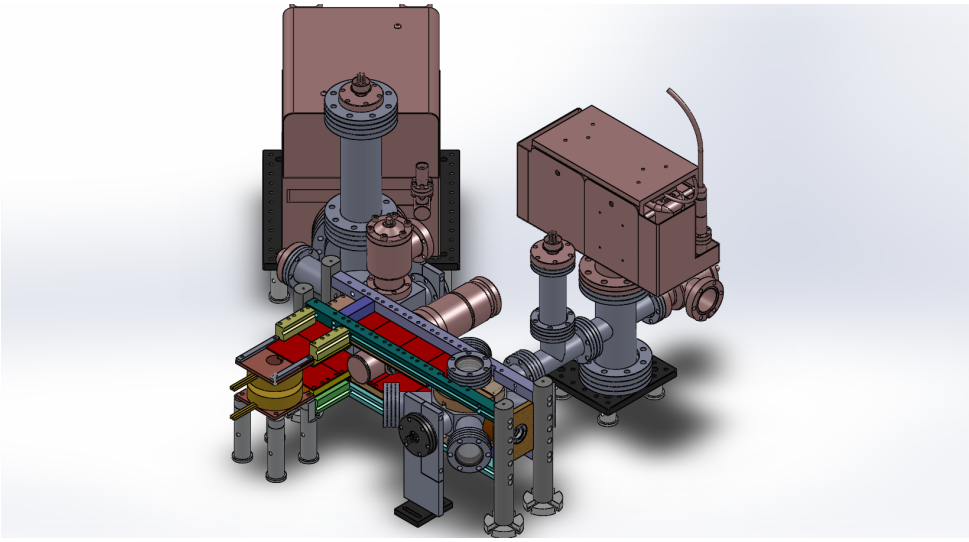

Figure 1: Experimental Apparatus - 2 vacuum cells connected by an L shaped tube.Transport between the cells is done with a magnetic transport system of 15 coil pairs (in red). An all metal gate valve (VAT 48124-CE01) is placed between the cells to allow keeping a high vacuum in the science cell when replacing the atom sources. MOT cell has 6 windows for MOT beams and 5 getters of ^{87}Rb and ^{40}K that provide the atoms for the experiment. Vacuum is maintained with 2 Ion pumps, another titanium sublimation pump is connected but was not used.

2.2 MOT Cell

2.2.1 Laser Cooling and MOT

The first steps in cooling atoms to quantum degeneracy is to capture the atoms, reduce their temperature using 'Doppler cooling' and increase their density in a Magneto Optical Trap (MOT) [23, 24]. This is done by utilizing a combination of magnetic fields and dissipative light forces. The magnitude of the scattering force light exerts on the atoms equals the rate at which the absorbed photons impart momentum to the atoms times the photons momentum [20] :

$$F_{scat} = \hbar k \frac{\Gamma}{2} \frac{I/I_{sat}}{1 + I/I_{sat} + 4\delta^2/\Gamma^2} \tag{3}$$

I - laser intensity, I_{sat}- saturation intensity ,δ - laser detuning from atomic resonance, Γ-natural linewidth, $\hbar k$ - photon momentum. To cool atoms in vacuum from room temperature to micro-Kelvin temperatures, we use 6 circularly polarized beams red detuned from resonance together with a weak linear magnetic field - a Magneto Optical Trap. When an atom is moving towards a beam it sees a larger laser frequency due to Doppler effect, and thus have a greater chance to absorb photons form that beam. The atom then dissipates the energy through spontaneous emission to all directions, so on average it losses some of its initial velocity and gets colder. Effectively the beams exerts a damping force on the atom with a viscosity constant $\alpha = 4\hbar k^2 \frac{I}{I_{sat}} \frac{-2\delta/\Gamma}{\left[1+4\delta^2/\Gamma^2\right]^2}$ [20], this technique is called Optical Molasses. To add a restoring force

to this and increase atomic density we use a magnetic field of the form $\mathbf{B} = b' \begin{pmatrix} x \\ y \\ -2z \end{pmatrix}$. The magnetic field is produced by 2 identical coils with a joint axis with current flowing in opposite directions (Anti-Helmholtz configuration). This magnetic field is not strong enough to trap the atoms at this stage, but due to the beams circular polarization it changes the selection rules for transitions between the Zeeman states and leads to an imbalance in the scattering force from the laser beams that push the atom back towards the center of the trap, so the cloud density increases.

The force exerted on an atom in a linear magnetic field with velocity v at a position z, shined by two counter propagating beams with circular polarization along the z axis is:

$$F_{MOT} = F_{scat}^{\sigma^+}(\omega - kv - (\omega_0 + \beta z)) - F_{scat}^{\sigma^-}(\omega + kv - (\omega_0 - \beta z)) \simeq -2\frac{\partial F}{\partial \omega}kv + 2\frac{\partial F}{\partial \omega_0}\beta z \quad (4)$$

$\pm kv$ - is the Doppler shift of an atom moving towards (opposite) a laser beam with wave vector k , $\beta z = \frac{g_f \mu_B}{h}\frac{dB}{dz}z$ - is the frequency shift due to Zeeman splitting for an atom at z.

In our apparatus we built a two-species MOT of bosonic (^{87}Rb) and fermionic (^{40}K) atoms by superimposing two pairs of trapping laser beams. At each pair, the first laser ('Cooling laser') is on a close cycling transition which performs the trapping and the cooling, while the second laser ('Repump laser') brings the atoms out of the lower ground state level to an excited level, from which they can return to the lower state of the cycling transition by spontaneous emission. For the ^{87}Rb and ^{40}K lasers we used two 780nm and 767nm External Cavity Diode Laser (ECDL) [25], respectively. These lasers are locked with polarization spectroscopy to the spectral lines corresponding to the cooling and repumping transitions. Because of the low natural abundance (0.0117%) of K^{40} [26], and the use of natural potassium cell in our locking system, its spectral lines cannot be observed. Therefore we locked our lasers to the K^{39} spectral lines and shift their frequency with Acousto-Optic Modulators (AOM) to the desirable transitions. The laser light is transferred by two single mode polarization maintaining fibers to the experiment. Afterward, we separate the beam to 6 beams (2 counter propagating beams in each axis), which form the MOT.

The magnetic field is generated by 2 coils made of 49 turns of copper wire with inner/outer radius $37/50mm$, and a distance $46mm$ between the coils along the joint axis z. We trap 2×10^9 ^{87}Rb atoms in the MOT with a loading time of $0.8sec$.

2.2.2 Magnetic Trap and Transport

We use our MOT coils to make a magnetic quadrupole trap with a potential $U_{MT} = b'\sqrt{x^2 + y^2 + 4z^2}$. This is done by turning off the MOT beams and increasing the current to produce an axial gradient $\left|\frac{dB}{dz}\right| = 2b' = 165\ \frac{G}{cm}$. The quadrupole trap is a linear trap with cylindrical symmetry, its confinement in the axial direction is twice the radial confinement $\frac{dB}{dz} = 2\left|\frac{dB}{dr}\right|$ and it has a zero

magnetic field in the center which could cause Majorana losses at sufficiently low temperatures. After Sisyphus cooling of the atoms from the MOT and optical pumping of the atoms to state $\left|F=2\, m_f=2\right\rangle$ we trap 0.9×10^9 atoms in the magnetic trap with phase space density $\sim10^{-7}$.

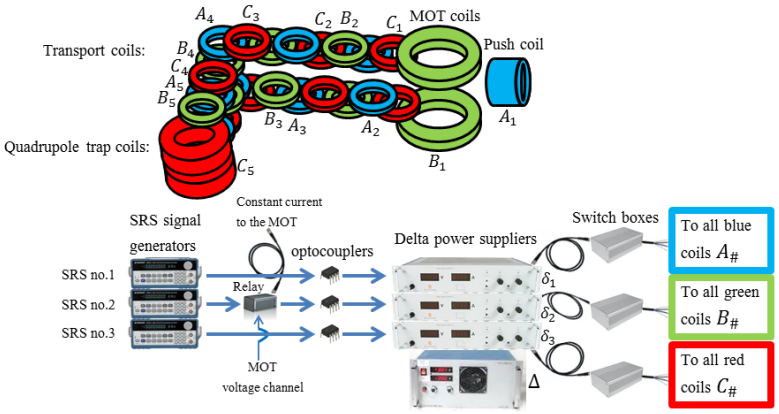

Figure 2: Magnetic Trap and Transport System - We use 3 function generators to control the currents in the MOT cell and magnetic transport. The currents functions are passed to 3 Delta power supplies ($\delta_{1,2,3}$) that generate the high currents in the coils one at a time. The switch boxes controls which coil is connected. At the end of the transport, the magnetic trap in the science cell is generated by a low noise power supply (Δ) that is connected directly to the computer.

We transfer the atoms along an L shaped tube with a diameter of $8mm$ and total length of $42cm$ to the science cell by a magnetic conveyor [19]. This method involves running currents in triplets of adjacent magnetic coil pairs consecutively to change the position of the magnetic trap along the path. We use 15 pairs of coils made of 34 turns of copper wire, with inner radius of $10mm$ and outer radius of $30mm$, the vertical distance between the coils is $47-72mm$, determined for each pair by technical constraints (they must overlap and cannot be put at the same distance everywhere). One push coil is placed horizontally, $60mm$ from the MOT in order to move the atoms towards the tube entrance (from technical reasons we cannot do this with the transfer coils), it consists of 121 turns with inner/outer radius of $18.5/30mm$ and a length of $40mm$. We ran extensive simulations to find the currents needed to form a trap with its center at each point along the path, using only 3 coil pairs simultaneously. The current function is produced by 3 function generators (SRS DS345), it is inserted to 3 power supplies (Delta SM 15-200 D) that generate the currents at each point. The power supplies are connected through switch boxes that controls which coils are connected. After the atoms are transferred to the science cell we switch between the last Delta power supply (δ_3 in figure 2) to a low noise power supply (Fug NTN 4200-12.5, Δ in figure 2) to get a more stable trap with less heating of the atoms, it also allows us to get tighter confinement (up to 660 $\frac{G}{cm}$ axial gradient). .

After optimizing the transport we got 3.2×10^8 atoms in the quadrupole trap in the science cell, with 35% transport efficiency. Most of the atoms are lost in the beginning of the transport

at the MOT cell where the pressure is higher and in the entrance to the science cell because it is smaller than the tube so the cloud edges are cut.

2.2.3 Imaging System

In the MOT cell we use fluorescence imaging [27], this is the simplest method of imaging cold atoms. We flash the atoms with the repump and cooler lasers from all 6 MOT beams $0.3ms$ with the cooler tuned to resonance for and collect the scattered photons to a CCD camera (PCO Pixelfly qe) placed in a 45° angle with respect to the horizontal MOT beams to avoid saturation.

We use a photo-diode to monitor the number of atoms loaded in the MOT and we calibrate our fluorescence imaging measurements to it.

2.3 Science Cell

2.3.1 Magnetic Trap

Magnetic coils in the science cell were planned for use at high currents to generate a tight magnetic quadrupole trap for evaporation process, and for tuning of interactions via Feshbach resonance [5] for ^{40}K atoms. The currents are generated by a low noise power supply with maximal output of $250Amp$ and $12.5Volt$, that can generate an axial magnetic gradient of 660 $\frac{G}{cm}$ (currents in opposite direction - anti-Helmholtz configuration) and a constant magnetic field to get to the ^{40}K Feshbach resonance at 202 G (currents in same direction - Helmholtz configuration) in the cell. The trap coils are made of 24 turns of hollow square $5mm$ copper tubing, the coils have an outer radius $40mm$ an inner radius of $15mm$. To keep the coils from heating we run cooling water through it. Fast switching of the coils is done by lowering the current in the power supply and directing it to high power resistor, this allows a shutdown time of less than $0.5ms$ and avoids any residual currents in the coils. The coils are positioned as close to the cell as possible, the distance between them is $14mm$. They were meant to produce a magnetic trap in the cell center but due to a misalignment of the cell by 3.5° the trap is located in the upper half of the cell, about 1.8 mm from the top wall.

To control the position of the trap at low currents and cancel external magnetic field we use another pair of coils in each axis, in the Helmholtz configuration. These coils are made of about 40 turns of thin copper wire and have a square shape with a side length of $24cm$.

2.3.2 Optical Plug

To avoid Majorana losses we use an optical plug to repel atoms from the center of the trap, using this method we don't need to add more coils to the system (as in a Ioffe-Pritchard trap [15]) so we maintain a high optical access to the cell. When light far from resonance interact with atoms, the scattering rate is small and the dominant force is the dipole force. The electric field of the laser **E** induces an electric dipole on the atoms **d** that oscillates with the same frequency. This

induced dipole then interact with the electric field, the interaction energy is [28]:

$$U_d(\mathbf{r}) = -\frac{3\pi c^3}{2\omega_0^3}\left(\frac{\Gamma}{\omega_0-\omega}+\frac{\Gamma}{\omega_0+\omega}\right)I(\mathbf{r}) \tag{5}$$

c - speed of light, ω_0 - atomic resonance, ω - laser angular frequency, Γ- natural linewidth of excited state and I is the laser intensity. For ^{87}Rb atoms shined with a Gaussian beam of $532nm$ wavelength and waist of $30\mu m$ (intensity falls to $1/e^2$) we get a potential maximum $U_0 = 42.3\frac{\mu K}{Watt}$ at the center of the beam.

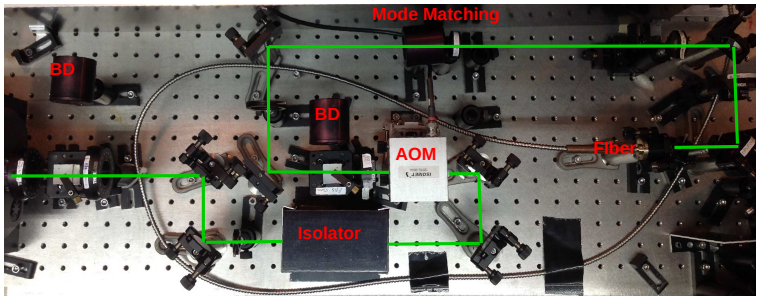

Figure 3: Optical Plug System - Our optical plug is produced from a 10 *Watt* laser that is passed through an isolator and an AOM, used for fast switch-off. We use a x2 telescope for spatial mode matching to a single mode optical fiber. Beam dumps (BD) are placed along the path to allow working at high power, because thermal lensing in the AOM changes the spatial mode.

The plug beam is generated by 10 Watt laser (Verdi-V10 of Coherent Systems) with a wavelength of $532nm$, the beam passes through an insulator (IO-5-532-HP Thorlabs) and a 40 MHz Acousto Optic Modulator (Isomet 1201E-964A) used for fast switch off. Due to thermal lensing in the AOM the beam changes its spatial mode considerably. To take it into account we had to work with high intensity laser at the AOM and deflect most of the power to a beam dump afterward. We use a telescope for mode matching before the beam goes through a single mode, polarization maintaining high power fiber (LMA-PM-15 NKT Photonics) to get a very clean spatial mode and better stability of the plug position. At the output of the fiber we connected a custom made focuser (60FC-SMA-T-23-M50L-26.mod Schafter-Kirchhoff) that produces a Gaussian beam with a waist of $30\mu m$ at $30cm$ distance from the focuser lens. To get a stable optical plug the focuser is mounted on a stable mount (IVM100 Siskyou) and it passes only 2 more mirrors before the cell (one of them dichroic to allow the imaging beam to pass). To control the position of the plug precisely we use a Picomotor piezo linear actuator (Newport 8302) mounted on one of the mirrors. The plug hits the cell from the bottom and is deflected to a beam dump above the cell with another dichroic mirror. A resonant imaging beam is coming from above the cell in opposite direction to the plug. It allows us to image the atoms and look at the effect of the plug on the atoms for accurate alignment without saturating the camera.

2.3.3 RF system

For RF induced evaporation of the atoms we use a single loop coil with a diameter of $4cm$ of made of a rectangle copper wire ($1.2 \times 2.5mm$) that acts as a directional antenna. The signal is generated by Tabor 8025 function generator that provides a clear sine signal in the range of 0-100 MHz from its Sine-Out output, we use a remote computer to control it in Arbitrary FM mode which allows precise control on the evaporation process. We use a switch and an amplifier of Mini Circuits (ZHL-3A+) to pass the signal to the coil. We put the coil as close to the cell as possible ($\sim 5cm$) and perpendicular to the trap axis to prevent coupling of the RF signal to the trap coils. We tested the transmitted the signal from this system using another smaller coil at a distance of $20cm$ and got a clean signal without any anti-resonances at our working frequency range.

2.3.4 Imaging System

In the science cell we intend to use a phase contrast imaging system [27] with high resolution ($\sim 1\mu m$) in the horizontal direction, however it is was not yet fully functioning at the time we made the measurements I present here. We have built an absorption imaging system in the vertical direction that was used to get all the data from the science cell presented in this thesis. Absorption imaging is done by shining the atoms with on resonance laser beam and imaging the shadow they cast on a CCD camera. Optical density is defined by Beer's law $I = I_0 e^{-OD}$, I_0, I are respectively the entering and emerging intensities from the atom cloud. Each measurement is made by 2 shots one with atoms and one only with the beam, the time between the 2 shots is $\sim 100ms$ to allow the atoms to spread away from the trap. From the 2 images we derive the optical density and calculate the column number density in each pixel - $n = \frac{OD}{\sigma}$,where σ is the absorption cross section for ^{87}Rb [29]. The imaging lens with $f = 150mm$ is placed at a distance of $2f$ from the cell and the CCD, the resolution of our absorption imaging system is $\sim 10\mu m$.

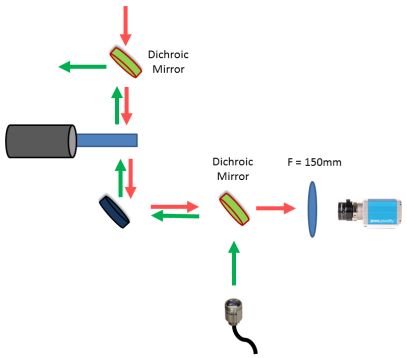

Figure 4: Layout of our Absorption Imaging System - Optical plug and imaging beam are both in the vertical axis but with opposite direction to enable aligning the plug using images of the atoms and avoid saturation of the camera. We use 2 dichroic mirrors to deflect the plug beam from the imaging system.

3 Results

3.1 Characterizing the Trap

Our trap is a hybrid trap of magnetic and optical forces, before adding the optical part we characterized the magnetic trap alone to get a measure of how good the vacuum is in the science cell and to see the effect of Majorana losses in cold clouds.

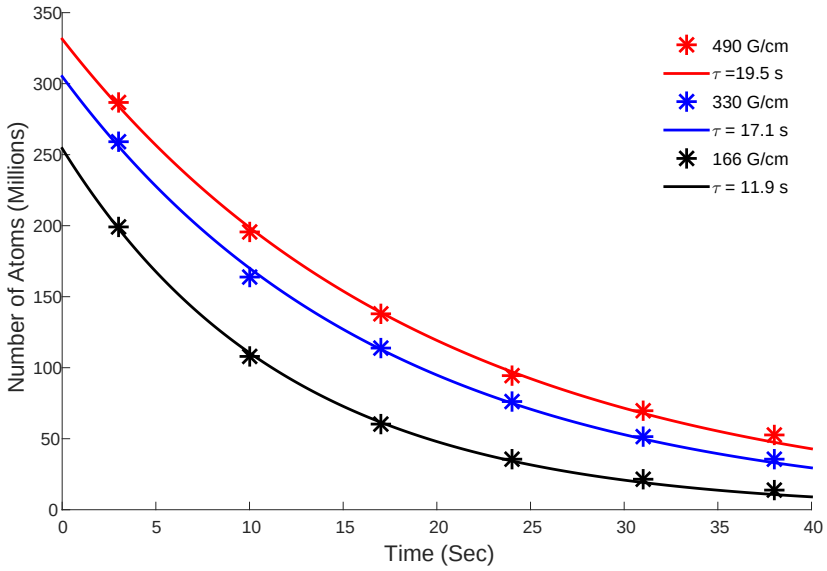

Figure 5: Life Time of Atoms in a Magnetic Trap - Number of atoms left in the magnetic trap without plug for different holding times. τ is the $\frac{1}{e}$ lifetime obtained from the exponential fit. Changing the magnetic axial gradient affects the lifetime of the atoms, which indicates the effect of another loss mechanism besides collisions with background gas.

Our measurements (figure5) show long lifetime of atoms in the trap, up to 19.5 seconds in a strong magnetic trap, which indicates a good vacuum separation of the science cell from the MOT cell where the lifetime in a magnetic trap is about a second (depending on how many atoms we release to the cell from the getters). We cannot measure accurately the temperature of the atoms immediately when they enter the science cell because the cloud size is comparable with the cell size and it hits the cell walls before we can measure its expansion rate. To approximate the temperature we can use the RF radiation, measuring at which frequency a significant loss of atoms occurs. Assuming it is of the order of $k_B T$ we get that the temperature is close to $1mK$ after we increase the axial magnetic gradient to $490\frac{G}{cm}$ and compress the atoms.

It is clearly visible in figure 5 that the lifetime has a strong dependence on the magnetic gradient. This indicates that collisions with background gas is not the only loss mechanism in the trap. Other possible mechanisms may be Majorana losses, light scattering or collisions with the walls of the cell, we think the later one is the relevant mechanism since Majorana losses should increase when the gradient is increased (eq. (2)) and light scattering should not be affected directly by the magnetic gradient.The cloud in this measurement is still relatively hot so

Majorana losses should not be an important factor. To verify that we repeated the measurement after aligning the optical plug and seeing its effect on cold clouds but got the same dependence on magnetic gradient as in figure 5. To prevent light scattering we covered our lasers table and our experiment table with curtains in all directions, we added mechanical shutters on the lasers table and during the holding time of the atoms in the trap we change the laser frequency to be 70 MHz off-resonance. With these methods we have a very good separation between the 2 tables and the probability of resonant photons to reach the cell is small.

From looking at pictures of large clouds we see that the hottest atoms are very close to touching the cell walls, specifically the upper wall, that will remove them from the trap. In the first second after the atoms reach science cell we see a faster decay. To check if it is the effect of the wall we decreased the size of the MOT beams, that gets less atoms in the MOT stage and less heating of the cloud when loading the atoms to the magnetic trap and transporting them. The cloud in the science cell after transport now has a lower temperature, less atoms and is smaller in size than before. Its distance from the wall is now greater than its size and the effect of the wall should be reduced. In figure 6 we show that the life time of the atoms in the trap increases significantly for smaller clouds, all in the same trap with a magnetic axial gradient of 490 $\frac{G}{cm}$ and without optical plug.

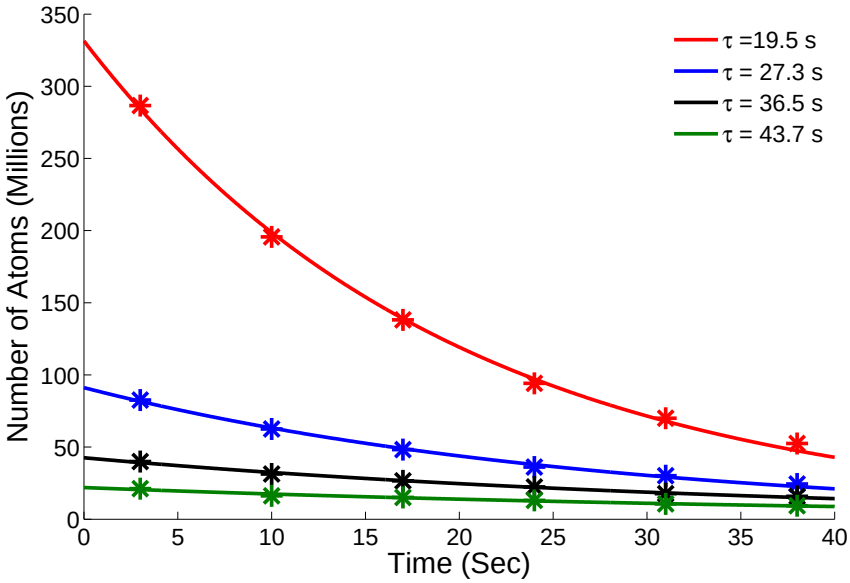

Figure 6: Cloud Size Effect on Life Time - Number of atoms left in the magnetic trap without optical plug for different holding times and exponential fits to the data. Changing the initial number of atoms and cloud size affects the life time of the atoms in the trap. The smaller the initial cloud is, it has a longer lifetime. Which can be attributed to atoms in large clouds colliding with the wall. All measurement were done with magnetic axial gradient of 490 $\frac{G}{cm}$.

Effectively the wall causes some uncontrolled evaporation in our trap by removing the hotter atoms from the trap, this will decrease the cloud temperature and size gradually as less and less atoms are able to get to the wall. At some point the cloud should get cold and small enough

that the wall effect will be negligible, but we do not see this change in our measurements and the dependence on magnetic gradient is relevant even for small clouds. This indicates that there is some heating mechanism of the atoms in the trap that causes the atoms to get away from the center and hit the wall. Magnetic traps are known to be noisy and can be affected by stray magnetic fields or noise from the power supply, we measured the heating of atoms in the trap (with optical plug) for very cold cloud and got a heating rate of $0.3\frac{\mu K}{Sec}$. While this gives some indication, it does not fully explain the lifetime dependence on magnetic gradient that we have measured.

3.2 Plugging the Trap

3.2.1 Aligning the Optical Plug

Aligning the plug is a delicate procedure. Our optical plug beam has a waist of $30\mu m$ that we need to align to the center of the trap where Majorana losses are significant, this hole in the trap is typically of the size of a few microns (see section 1.2.1) .

First we align the plug roughly to center of the magnetic coils using a physical target that marks the center. This allows us to hit a large cloud in some point and use the atoms for alignment. To see the effect on the atoms we inject a weak resonant beam ($780nm$ wavelength) to the same fiber with the plug beam and turn it on with the absorption imaging beam, the high intensity ($\gg I_{sat}$) resonance light on the atoms makes the atoms invisible to the imaging beam and leaves a dark spot in the image, marking the plug position. After aligning the red beam to the center of the cloud we turn it off and shine only the plug beam on the atoms. To see its effect we use RF evaporation to get a smaller cloud and release it from the trap to get lower density so the plug effect has better contrast, we leave the plug on during imaging process and the atoms are repelled from the plug and we can see a hole (see figure 7.a). We align the hole to the center pf the cloud.

To get an exact position of the trap center we take *in situ* images of a small cloud (after evaporation) with a very strong magnetic field. It is very important to make sure the cloud is not moving when we use weaker magnetic traps, which are necessary for deep evaporation when the plug is most significant (see figure 10). To do that we take *in situ* images of the atoms in weak magnetic gradient and compare the centers of the cloud to the one we found with strong magnetic gradient. To move the center of the weak trap we use 3 orthogonal pairs of compensation coils in Helmholtz configuration that generate constant magnetic field in the cell. After adjusting the weak magnetic trap to be in the same position as the strong magnetic trap we align the plug beam to the same center. The final step is looking at *in situ* measurements with the plug of a very cold cloud and seeing that it has the shape of a symmetric ring around the center (see figure 7(b)).

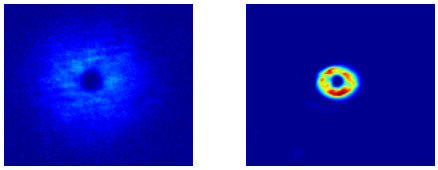

(a) (b)

Figure 7: Imaging the Plug with the Atoms - To find the exact position of the plug we look at the atoms, first we look at larger clouds at low densities after release from the trap **(a)** and then in the magnetic trap to see a symmetric ring **(b)**. Picture area $0.4mm^2$.

3.2.2 Controlling Trap Shape

A ring trap is not a good one to achieve BEC. The trap does not have one clear minimal point where the atoms accumulate, they spread over a larger area and the density is lower. In addition, the trap is not an ideal harmonic trap, making it harder to measure properties of the condensate (chemical potential, phase space density). Using the known properties of the optical plug beam and the magnetic field we can calculate the potential to see how it changes when we move the plug and calculate properties of the minimal point (Figure 8).

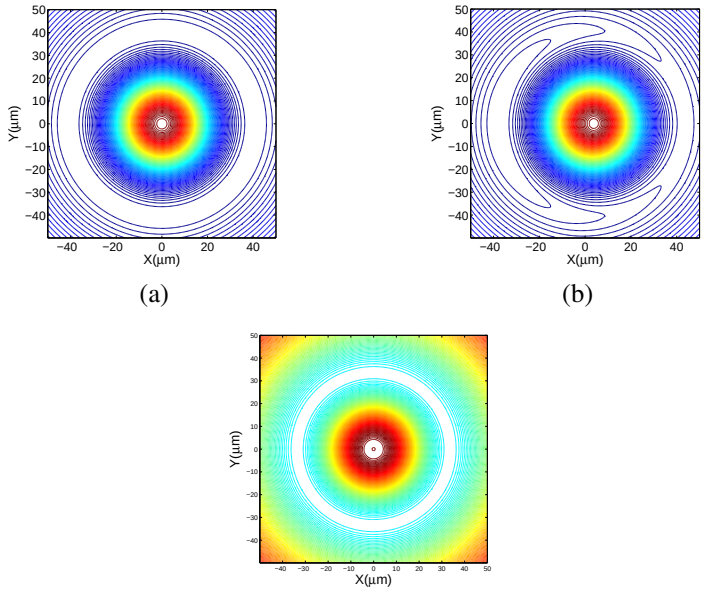

(a) (b)

(c)

Figure 8: Calculated potential change with plug movement - calculated equipotential lines with plug centered **(a,c)** and moved to the right by $3\mu m$ **(b)**. Plug power is $3.1Watt$ **(a-c)**, axial magnetic gradient is $181\frac{G}{cm}$ in **(a,b)** and $480\frac{G}{cm}$ in **(c)**. Even a small movement (less than 10% of the optical plug spot size) is enough for a minimal point to be formed and change the clouds position at low temperatures. In **(a,b)** the lines are much denser close to the center in the optical potential than in the outer part of magnetic potential, showing the unharmonicity of the trap. For a strong trap, the confinement around the minimum is tighter but the plug barrier compared to minimum is lower. Calculated width of cloud and potential in the 3rd dimension (vertical axis) is of the same order of magnitude as in radial direction.

We can explore the properties of the calculated potential to get the trap most suitable to the evaporation process and produce BECs consistently. To calibrate and verify our calculation and compare it to the apparatus we first look to find when the magnetic field overcomes gravity and a trap is formed, i.e. $\mu_B g_f m_f \frac{dB}{dZ} = m_{Rb} g$, the calculated axial gradient is $15\frac{G}{cm}$. Looking at the atoms in the trap we saw that at an axial gradient below $14.8 \pm 1.5\ \frac{G}{cm}$ the atoms are lost from the trap, in agreement with the calculation. A second test is the RF frequency required to evaporate all atoms from the trap at different gradients and plug position, to calculate this we find the Zeeman splitting at the trap minimum for each case (figure 9). Comparing the measured value in axial gradient of $181\frac{G}{cm}$ shows excellent agreement with calculation (less than 2% difference). This calculation also demonstrates the importance of plug stability to get BEC consistently, a change of $5\mu m$ in plug position (smaller than our imaging resolution) generates a change of more than 10% in minimal evaporation frequency, which will lead to a different cloud temperature and condensate fraction for the same evaporation process.

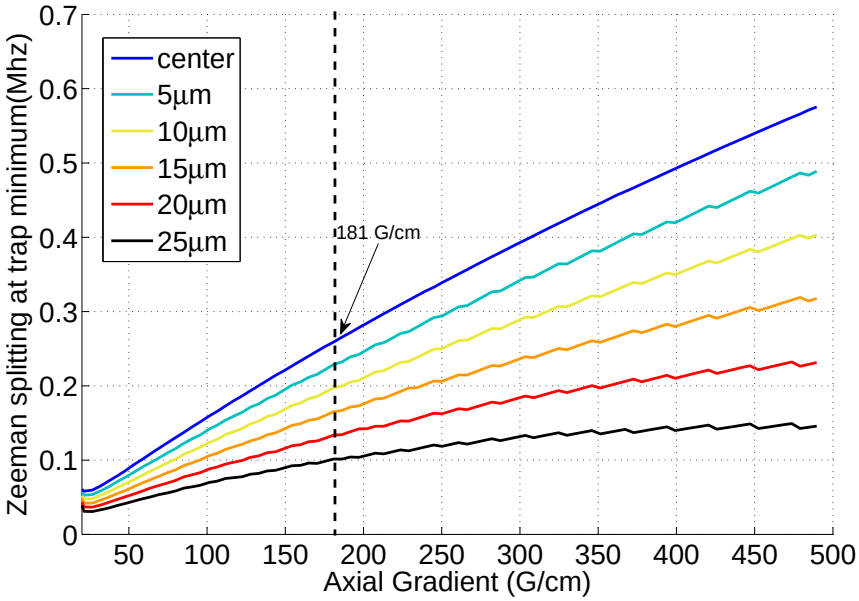

Figure 9: Effect of Plug Position - Change of Zeeman splitting at trap minimum when the plug is miss aligned (colors). The minimal Zeeman splitting is the lowest frequency we can get to in the evaporation. It is shown that small movements, on the scale of our imaging resolution, can change the trap properties and affect the evaporation process.

Another important property of the trap is the optical plug power, we calculate its effect on the potential barrier at the center of the trap for different magnetic gradients and its effect on the minimal evaporation frequency (Figure 10). The results show that a power of $1.8 Watt$ is sufficient to produce a potential barrier for all magnetic gradients for temperatures below $30\mu K$ where Majorana losses are significant.

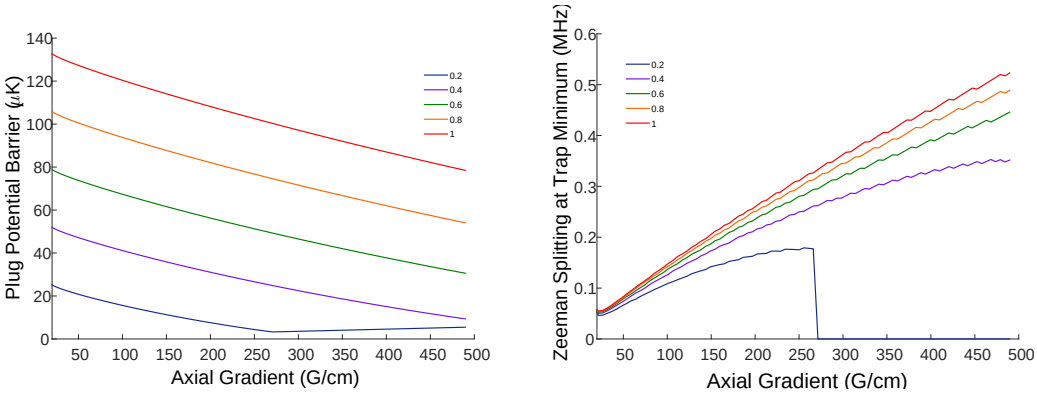

(a) (b)

Figure 10: Effect of Plug Power - **(a)** Potential barrier produced by the plug, relative to the trap minimum.**(b)** Zeeman splitting of atoms at the trap minimum. Colors indicate different plug power (relative to 3.1$Watt$ - maximum). It is clear that the plug produces a sufficient potential barrier even at 0.6 of the maximum power. The magnetic axial gradient lowers the effective barrier and changes the minimal frequency for the RF evaporation. At 0.2 power, the trap breaks down when the gradient is too strong and the plug becomes negligible.

We want to have a stable trap with one clear minimal point where the atoms accumulate. To achieve that we break the symmetry of the trap by moving the plug a few μm off-center, and then use the evaporation to cool the cloud to a low temperature where the plug is significant but well above the critical temperature of a BEC. Looking at the *in situ* images we can see that the trap changes from a symmetrical shape (figure 11 (f)) to an a-symmetrical shape with a clear minimum (figure 11 (a,b)), when the plug is misaligned Majorana losses are significant and less atoms are left in the trap but we can still find a good working position where most atoms are left in the trap and a clear minimum is formed (figure 11 (c)). After deep evaporation at much lower temperatures when a BEC is formed we can see more than one minimum (figure 12 (a-c)). This is the result of the imperfections of the trap (beam shape, coils, plug position) that are more significant at lower temperatures. Precise control of the plug position allows us to produce a stable and controllable minimal point where a consistent BEC is formed (figure 12 (d-f)).

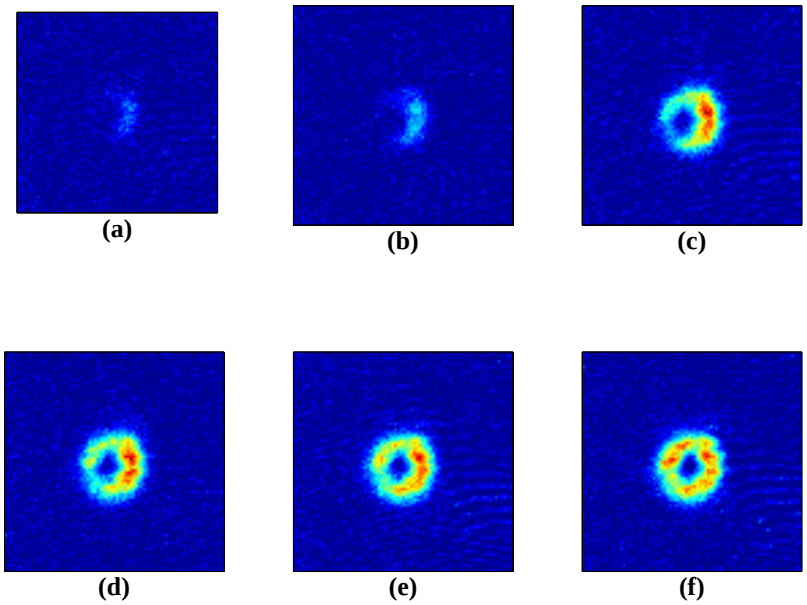

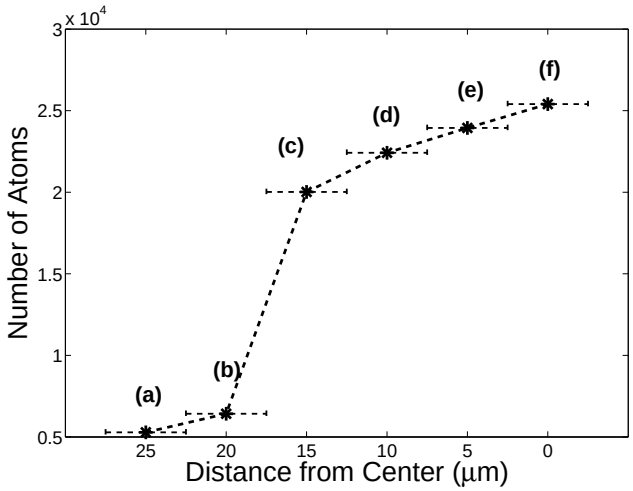

Figure 11: Moving the Plug to Produce a Distinct Minimal Point - The atoms tend towards one minimal point as the plug is move away from the center. The number of atoms is decreased due to Majorana losses when the plug is misaligned.

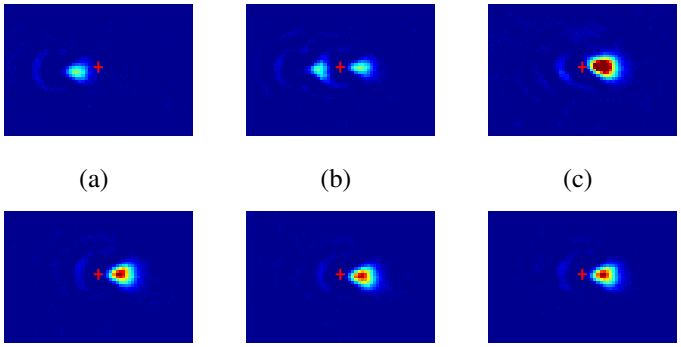

(a) (b) (c)

(d) (e) (f)

Figure 12: Trap Stability - Trapped atomic clouds (*in situ*) at the end of evaporation in consecutive measurements, all but plug position is the same (evaporation process, trap strength etc.). **(a-c)** The Plug is centered, but the cloud randomly chooses its position between 2 minimal points, it can even split to 2 clouds **(b)**. **(d-f)** The Plug is deliberately off-centered a few μm to the left, the cloud is always in the same position indicating a stable minimum potential point. Red cross indicates magnetic center for reference.

3.2.3 Preventing Majorana losses

To see that our plug is preventing Majorana losses we evaporate as deep as possible with and without the plug and count the number of atoms after release from the trap (figure 13). This was the first evidence that the plug is preventing Majorana losses during the evaporation process and it allowed us to continue the evaporation to quantum degeneracy.

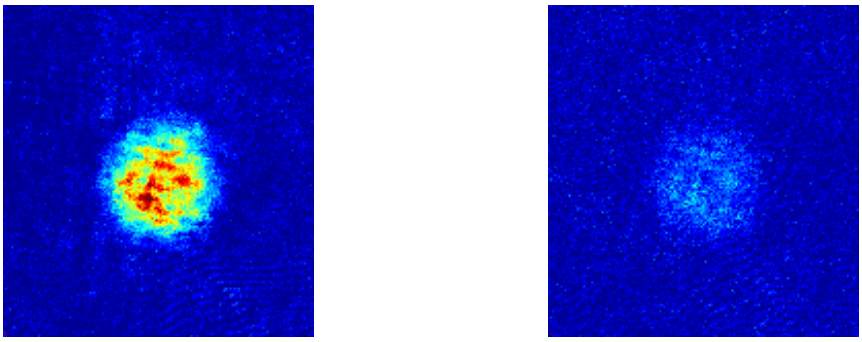

(a) (b)

Figure 13: Plug Effect after Evaporation - evaporation from 40 MHz to 0.5 MHz in 25 sec, pictures are 2.5ms after release **(a)** 72×10^3 atoms with the plug ON during evaporation and **(b)** 22×10^3 atoms without plug during evaporation, it is clear that the optical plug prevents Majorana losses during the evaporation process. Each photo is average of 15 measurements, Picture area $0.8 mm^2$.

3.3 Evaporative Cooling

Our evaporative cooling process is done by holding the atoms in a tight magnetic trap with high collision rate and applying RF radiation on the cloud using a one loop coil antenna. We start the evaporation with a cloud of 3.2×10^8 ^{87}Rb atoms, in a magnetic trap with a strong axial gradient of 490 $\frac{G}{cm}$. We evaporate the atoms sweeping the RF radiation from 90 MHz to 2 MHz in 10 seconds with a linear ramp, then we reduce the axial gradient to $181\frac{G}{cm}$ and evaporate to lower frequencies (0.5-0.28 MHz) in 2 seconds with an exponential ramp with a time constant of 1.5 sec. Reducing the gradient is done in order to increase the potential barrier of the plug (see fig 10) and prevent Majorana losses, without it we were not able to produce a BEC.

We have worked on the evaporation process for a long time, changing evaporation rates, magnetic gradients, RF antennas and amplifiers, the most significant parameter for us was the number of atoms in the magnetic trap at the start of evaporation. When we got more than $\sim 3 \times 10^8$ atoms in the trap we were able to get an efficient evaporation process and a BEC was formed. With more atoms in the trap the collision rate is higher which allows a fast thermalization of the cloud and the density increases significantly during the evaporation process ("runaway evaporation"). With a lower number of atoms we were able to get to low temperatures but the density remained low and high phase space density was not achieved.

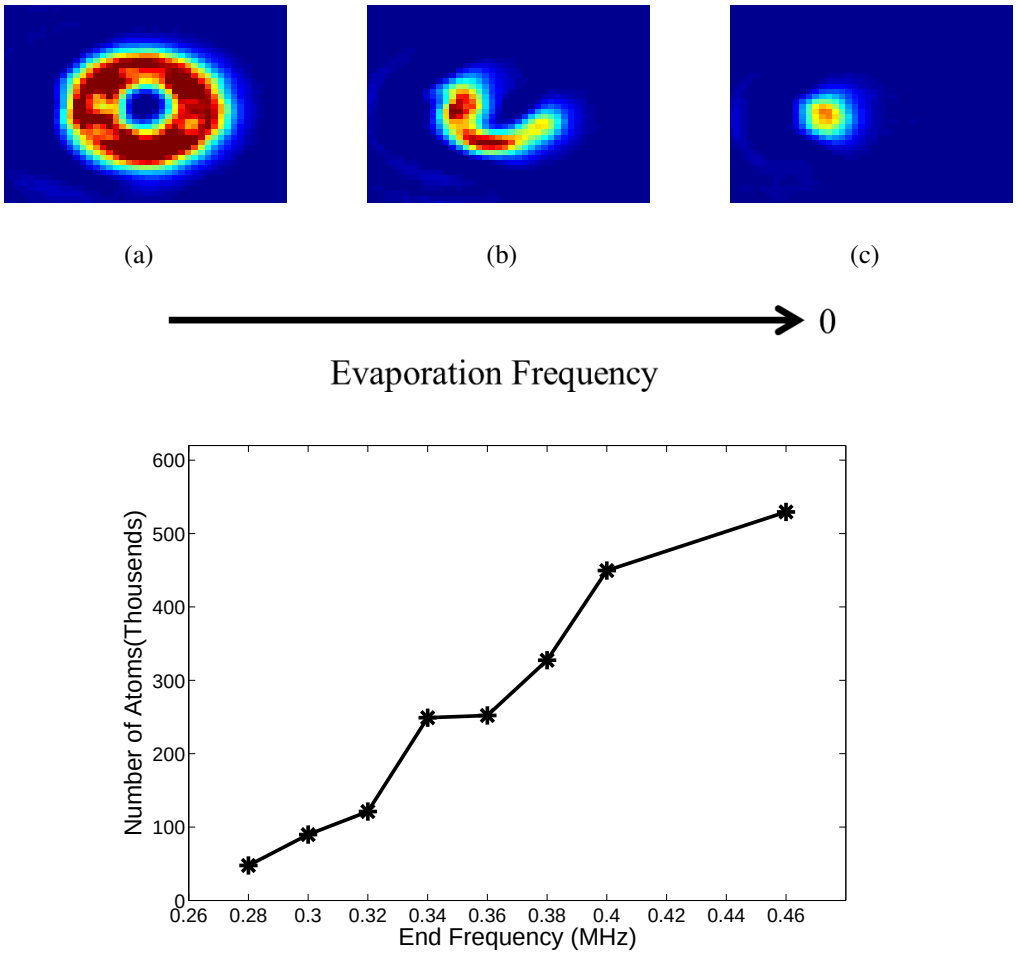

Figure 14: Evolution During Evaporation - **(a-c)** *in situ* images of the cloud at different stages of a evaporation,**(a)** at high frequency it has a symmetric ring shape, **(b)** it breaks down during evaporation until **(c)** all atoms are very close to one minimum point. **(d)** The number of atoms in the trap decreases as we change the final frequency in the last steps of evaporation. BEC is achieved roughly at $0.35MHz$.

3.4 Bose-Einstein Condensate

3.4.1 Observing BEC

The clearest indication of BEC is the appearance of a sharp peak in the atoms distribution after a long time of flight, this shows the macroscopic occupation number of the ground state of the system. These atoms have low momentum and they don't expand during the time of flight. The transition from a thermal cloud to BEC is shown in figure 15 ,when the cloud is below the critical temperature we see a high density of atoms that grows when we continue evaporating until we get an almost pure condensate.

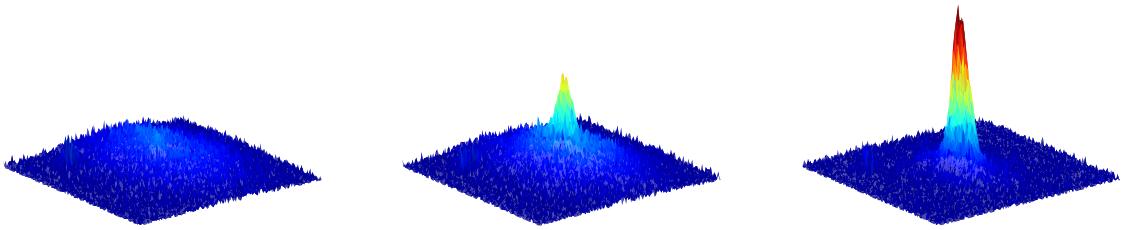

Figure 15: Bose-Einstein Condensation - Lowering the final frequency in the evaporation process (left to right), more atoms are occupying the ground state until almost pure BEC cloud is formed.

Another indication of BEC is the expansion of the cloud after release from an anisotropic trap. Unlike a normal cloud the BEC expands anisotropically, expansion in the strong confinement direction is faster than in the other directions so a cigar-shaped cloud turns into a disc-shaped cloud. The cloud in our trap is not exactly a cigar-shaped cloud and as I mentioned and controlling the shape of the trap in the smaller scales is difficult, but we can still clearly identify an anisotropic expansion below the critical temperature (figure 16).

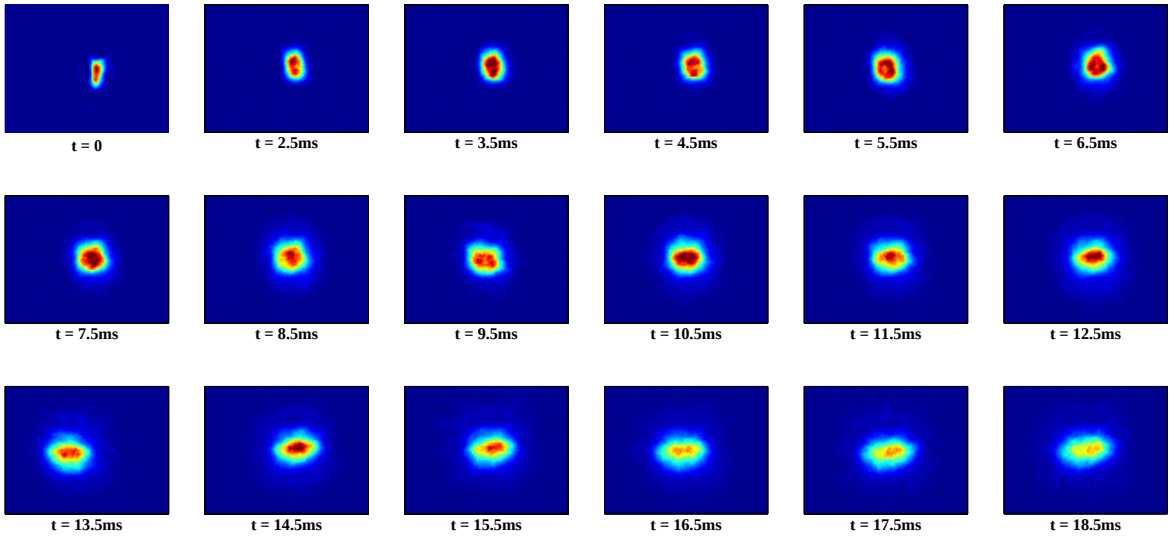

Figure 16: Anisotropic Expansion - Expansion of a BEC after deep evaporation, t is the time of flight. In the trap the cloud has an elongated shape along one direction ($t = 0$ *in situ*) and during expansion it flips its axis and becomes elongated in the other direction for $t \geq 12ms$

While our trap is not cylindrically symmetric we know from our potential calculations it has a stronger confinement in the radial and vertical directions than in the azimuthal direction, the aspect ratio is 8.6. That is also clearly visible in the *in situ* image of figure 16 . The anisotropic expansion is another indication that the cloud is cigar shaped. This allows us to calculate the

chemical potential of the condensate directly from its expansion [15]:

$$\mu = \frac{1}{2} m \frac{\omega^2}{1 + t^2 \omega^2} x_c^2 \tag{6}$$

where ω is the trap frequency along its strong axis, x_c is the half-length of the cloud in the same direction and m is the atoms mass. For long expansion time $t \gg \frac{1}{\omega}$ we can approximate $\mu \approx \frac{1}{2} m \frac{x_c^2}{t^2}$.

When atomic interactions in a BEC are very strong, the kinetic energy of the atoms can be neglected (Thomas-Fermi limit). This is valid when $u = \frac{8\pi a N_0}{a_\perp} \gg 1$ [30] where N_0 is the number of condensed atoms, a is the S-wave scattering length and $a_\perp$ is the cloud size in the tightly confined axis. At this limit, the chemical potential is [15]:

$$\mu_{TF} = \frac{1}{2} \left(15 \hbar^2 m^{1/2} N_0 \bar{\omega}^3 a \right)^{\frac{2}{5}} \tag{7}$$

where $\bar{\omega}$ is the geometrical average of the trap frequencies. We approximate the trap frequencies from our calculated potential and calculate $\mu_{TF} = 4.5\ kHz$ for a pure BEC with $N_0 = 1.2 \times 10^5$ atoms and scattering length $a_{Rb} = 110 a_0$ [31].

From expansion measurements we get $\mu = 3.2 \pm 0.2\ kHz$. The trap frequencies, especially in the angular direction, have a strong dependence on the plug position. Since we do not know the exact position of the plug, this can be a reason for the difference between the 2 results.

3.4.2 Fitting Bimodal Distributions

Characterizing the BEC is done by looking at the bimodal distribution of the expanding cloud after integrating in one direction (Figure 17). The condensate has a parabolic distribution (in the Thomas-Fermi limit) and by looking at its radius we can determine the chemical potential. The thermal cloud has a Gaussian distribution and by looking at its width and its expansion we can calculate the temperature of the cloud. By comparing the area below the 2 parts we can get the condensate fraction. The bimodal distribution is a better fit when there is a clear thermal and condensate part, that makes pure condensates harder to measure and it requires a long expansion time for the thermal cloud to be visible.

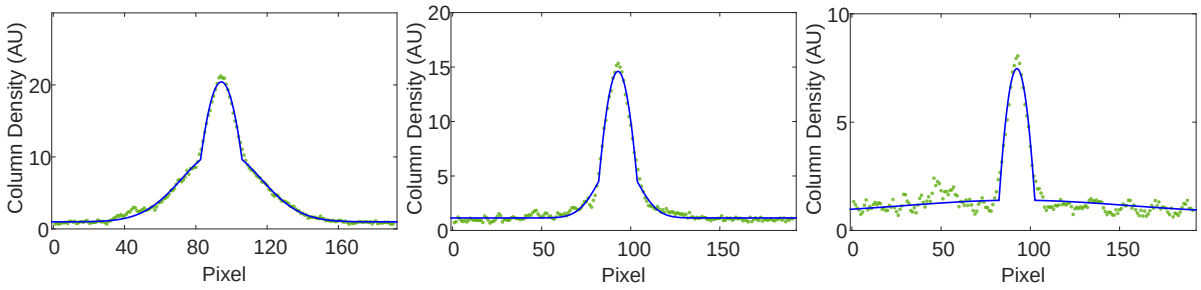

Figure 17: Bimodal Distributions - Column densities of the cloud after $22ms$ time of flight, integrating in one direction. Lowering the final evaporation frequency$(\mathbf{a} \rightarrow \mathbf{c})$ increases the number of atoms in the condensate until the thermal cloud is comparable to the noise level. **(a)** $\frac{N_0}{N} \sim 21\%$ **,**$T \sim 0.3\mu K$ **(b)** $\frac{N_0}{N} \sim \%43$ **,**$T \sim 0.1\mu K$ **(c)** no thermal cloud is visible.

Measuring the temperature of a BEC is done by fitting a Gaussian to the tails of the thermal cloud since the center of it is overlapping with the condensate. This makes the signal to noise ratio lower for BEC with a high condensate fraction and measuring the expansion of the cloud at different expansion times to get a linear fit is difficult. To overcome that we want to measure the thermal cloud in a single expansion time and calculate the cloud temperature from it, neglecting the initial cloud size. To verify that it is negligible we measured the cloud width at different times after release and compared the temperature from the linear fit to the one we got from every shot (Fig 18). We can see that in the first few shots the thermal cloud is not big enough and the initial size is important but after about $15ms$ measuring at one expansion time is good enough to determine the temperature and the initial size is negligible.

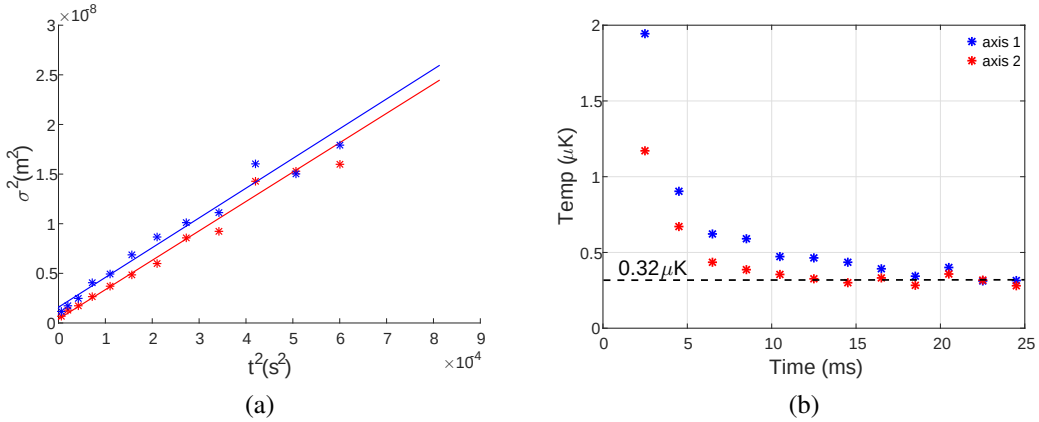

Figure 18: Temperature Measurement of a BEC - (a) Expansion of the thermal cloud tails in the 2 horizontal axes for a BEC with condensate fraction of 17%. σ is the width of the Gaussian thermal cloud, t is the time after release from trap. The linear fit is a good approximation and we get a temperature of $0.32\mu K$. (b) We calculate the temperature from each measurement alone (neglecting the initial cloud size) and compare it to the temperature from the linear fit (indicated by the dashed line). The temperature converges towards the line, and we can see that the contribution of the initial size of the cloud is negligible after $15ms$ of expansion.

3.4.3 Phase Space Density

Bose-Einstein condensation in ultracold atoms requires cooling the atoms until their de-Broglie wavelength is comparable to the inter-atomic distance. Phase space density is a single parameter that takes into account both these quantities - $\rho_{PSD} = n_0\lambda_{dB}^3$, where n_0 is the maximal density of the atoms in the trap, and $\lambda_{dB} = \sqrt{\frac{2\pi\hbar^2}{mk_BT}}$ is the thermal de-Broglie wavelength. At the end of the evaporation process the phase space density should be 1 for a BEC in a uniform potential, in an ideal 3D harmonic trap it should be 2.612 [15].

Calculating phase space density of the cloud requires measuring the temperature and density of the cloud in the trap. Our trap has a strange shape with a linear magnetic potential and a Gaussian optical potential making it hard to compare it to a standard harmonic trap like in a dipole trap or Ioffe-Pritchard magnetic trap. In the previous section I have shown we can measure the temperature of a BEC, but measuring its initial density is more complicated, we need to measure the number of atoms and then estimate in some way the size of the cloud in the trap. Measuring the number of atoms for a dense cloud must be done after releasing it from the trap and letting it expand (see figure 19) to avoid errors due to the high optical density. At high optical densities the intensity of the light that passes through the cloud is very low, so the signal to noise ratio is small and even for very little amount of light that get to the camera (e.g. scattered light, or off-resonant light) changes the measured number of atoms by much. One useful method for measuring the size of the cloud in the trap is by interpolating the linear fit from time of flight measurements to $t = 0$, assuming the cloud is close to a Gaussian shape in the trap (as in an harmonic trap) we can get the size of the cloud at $t = 0$ and calculate the average density in the trap. We have verified this method to be in agreement within a factor of 2 with *in situ* measurements for hotter clouds where the atoms have higher energy than the plug. Under these conditions the plug is negligible and the trap is linear. This means the atoms distribution is exponential and not Gaussian but it is still a good estimation. For colder atoms the plug is very significant, the Gaussian approximation is not valid and this method fails.

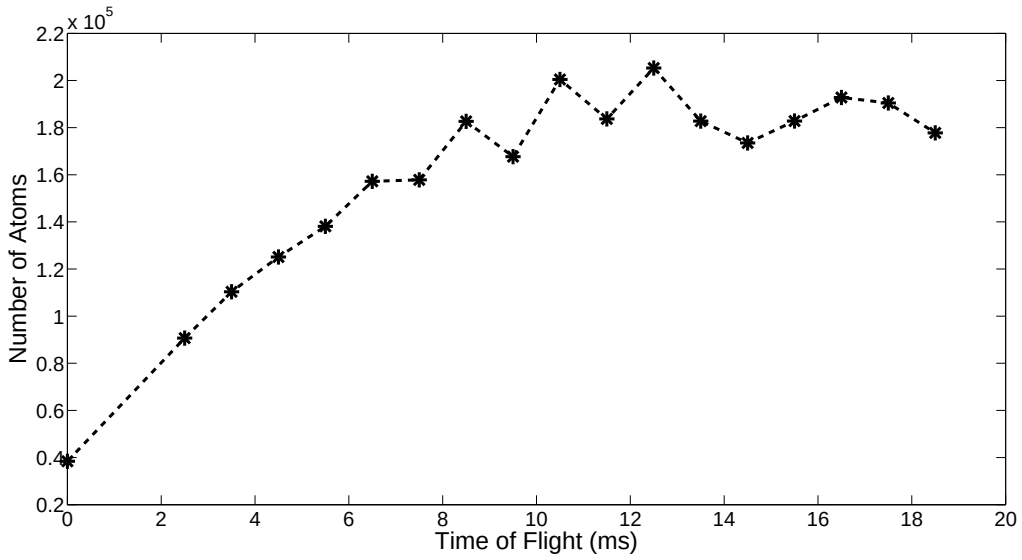

Figure 19: Number of Atoms During Cloud Expansion - Number of atoms of BEC measured from absorption imaging after release from the trap (first measurement is *in situ*). At first the cloud is too dense and we cannot see all the atoms due to high optical density (> 3), only after several milliseconds of expansion we can measure the correct number of atoms as it reaches a plateau at $\sim 1.8 \times 10^5$. Measurements were done after 8 seconds of evaporation to BEC.

We tried 2 other methods to calculate the density for very cold clouds: (1) Taking *in situ* images of the cloud. (2) Using a calculated potential with the measured temperature and number of atoms to calculate the probability distribution of atoms in space and peak density. *In situ* measurements did not provide good results because they show a lower number of atoms due to high optical density, and the cloud size is comparable with our optical resolution making it impossible to be measured accurately.

To calculate the potential we used the measured properties of the plug and magnetic gradient to calculate the probability distribution of the cloud according to the temperature measured in the cloud expansion. To get the peak density we multiply the measured number of atoms by the highest probability calculated. Using this method for a BEC close to the transition temperature (as was seen by the bimodal distribution after a long time of flight) we get a phase space density of 3.94, which is in a reasonable agreement with the theoretical value at the critical temperature 2.612. In reverse, this agreement validates the consistency of our methods for measuring thermodynamic properties of the trapped atoms, namely number of atoms, density and temperature.

N	165×10^3
T	$0.32\mu K$
$\frac{N_0}{N}$	17%
n_0	$1.1 \times 10^{14} cm^{-3}$
ρ_{PSD}	3.94
σ_{ring}	$3\mu m$
R_{ring}	$40\mu m$

Table 1: Phase Space Density Calculation Close to T_c - The temperature, number of atoms and condensate fraction were measured, the other quantities were calculated using the calculated potential and atoms distribution. The calculated value of ρ_{PSD} is in close agreement with the theoretical value for an ideal 3D harmonic trap 2.612 at T_c[15].

3.4.4 Protecting BEC

We already know from previous measurements that the heating rate in our trap is large compared to the condensate temperature, but we can still maintain a BEC for longer times ($> 0.5s$) by keeping the RF radiation ON at the final evaporation frequency after evaporation. Then we will have a very shallow trap, all the heated atoms will be removed from the trap by induced RF transitions and the BEC will be diminished but it will survive for a longer time. In figure 20 we show this effect on the BEC $0.5s$ after the end of evaporation with and without RF. We have also repeated this measurement when raising the frequency at the end of evaporation, less atoms were lost than without RF, the BEC was lost and the cloud was heated to a lesser extent as expected.

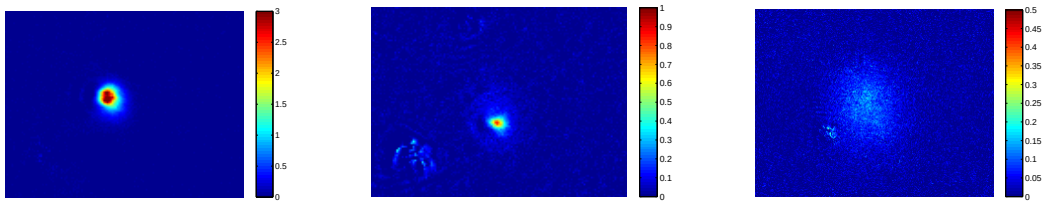

(a) (b) (c)

Figure 20: Heating effect on BEC - **(a)** 93×10^3 atoms in a BEC at the end of evaporation. **(b)** 20.3×10^3 atoms in a BEC held in the trap 0.5 second after the end of evaporation with RF and **(c)** 95×10^3atoms in a thermal cloud without RF. The RF radiation conserves the BEC for a longer time by removing the heated atoms from the trap. Without RF radiation the atoms are heated but stay trapped and the cloud losses its coherence and becomes thermal. All measurements are after $7ms$ time of flight, color scale indicates optical density. Picture area is $0.4mm^2$.

4 Conclusion

We achieved a Bose-Einstein Condensate in an optically plugged magnetic trap. Majorana losses were prevented by the optical dipole force exerted on the atoms at the center of the trap by our optical plug system. Efficient evaporative cooling was performed by RF induced evaporation in the hybrid trap, high phase space density was achieved consistently. We have characterized our BEC, measuring its temperature, phase space density and chemical potential. The good agreement with the theory for the critical phase space density and chemical potential validates our calculation of the potential with the optical plug and magnetic gradient. More precise measurements were not done because we wanted to continue our effort to produce a degenerate Fermi gas of ^{40}K, which was the main motivation to building the system.

Our system is still not completely assembled, but we have successfully showed the main capabilities required to produce a degenerate Fermi gas and fermionic superfluid, namely: capturing and cooling ^{87}Rb and ^{40}K in a MOT, transporting ^{87}Rb with magnetic transport from the MOT cell to the science cell, capturing the ^{87}Rb in a magnetic trap with a long lifetime in the science cell and evaporative cooling of the ^{87}Rb to quantum degeneracy. We have preliminary results of loading the cold ^{87}Rb cloud to a crossed dipole trap with high efficiency ($> 50\%$), the dipole trap is a favorable trap in terms of noise, stability and harmonicity which have limited us in measuring the properties of the BEC. Our next goals are repeating the whole process with ^{40}K cooled via sympathetic cooling and achieving a degenerate Fermi gas.

References

[1] Steven Chu, Leo Hollberg, John E Bjorkholm, Alex Cable, and Arthur Ashkin. Three-dimensional viscous confinement and cooling of atoms by resonance radiation pressure. *Physical Review Letters*, 55(1):48, 1985.

[2] Steven Chu. The manipulation of neutral particles.

[3] M. H. Anderson, J. R. Ensher, M. R. Matthews, C. E. Wieman, and E. A. Cornell. Observation of bose-einstein condensation in a dilute atomic vapor. *Science*, 269(5221):198–201, 1995.

[4] K. B. Davis, M. O. Mewes, M. R. Andrews, N. J. van Druten, D. S. Durfee, D. M. Kurn, and W. Ketterle. Bose-einstein condensation in a gas of sodium atoms. *Phys. Rev. Lett.*, 75(22):3969–3973, Nov 1995.

[5] Ph Courteille, RS Freeland, DJ Heinzen, FA Van Abeelen, and BJ Verhaar. Observation of a feshbach resonance in cold atom scattering. *Physical review letters*, 81(1):69, 1998.

[6] S Inouye, MR Andrews, J Stenger, H-J Miesner, DM Stamper-Kurn, and W Ketterle. Observation of feshbach resonances in a bose–einstein condensate. *Nature*, 392(6672):151–154, 1998.

[7] Markus Greiner, Olaf Mandel, Tilman Esslinger, Theodor W Hänsch, and Immanuel Bloch. Quantum phase transition from a superfluid to a mott insulator in a gas of ultracold atoms. *Nature*, 415(6867):39–44, 2002.

[8] DS Naik and C Raman. Optically plugged quadrupole trap for bose-einstein condensates. *Physical Review A*, 71(3):033617, 2005.

[9] Romain Dubessy, Karina Merloti, Laurent Longchambon, P-E Pottie, Thomas Liennard, Aurélien Perrin, Vincent Lorent, and Hélène Perrin. Rubidium-87 bose-einstein condensate in an optically plugged quadrupole trap. *Physical Review A*, 85(1):013643, 2012.

[10] Ettore Majorana. Atomi orientati in campo magnetico variabile. *Il Nuovo Cimento (1924-1942)*, 9(2):43–50, 1932.

[11] Wolfgang Ketterle and NJ Van Druten. Evaporative cooling of trapped atoms. *Advances in atomic, molecular, and optical physics*, 37:181–236, 1996.

[12] Markus Greiner, Cindy A Regal, and Deborah S Jin. Emergence of a molecular bose–einstein condensate from a fermi gas. *Nature*, 426(6966):537–540, 2003.

[13] Martin W Zwierlein, Jamil R Abo-Shaeer, Andre Schirotzek, Christian H Schunck, and Wolfgang Ketterle. Vortices and superfluidity in a strongly interacting fermi gas. *Nature*, 435(7045):1047–1051, 2005.

[14] Richard P Feynman. Simulating physics with computers. *International journal of theoretical physics*, 21(6):467–488, 1982.

[15] W Ketterle, DS Durfee, and DM Stamper-Kurn. Making, probing and understanding bose-einstein condensates. *arXiv preprint cond-mat/9904034*, 5, 1999.

[16] Wolfgang Ketterle, Kendall B Davis, Michael A Joffe, Alex Martin, and David E Pritchard. High densities of cold atoms in a dark spontaneous-force optical trap. *Physical review letters*, 70(15):2253, 1993.

[17] Jean Dalibard and Claude Cohen-Tannoudji. Laser cooling below the doppler limit by polarization gradients: simple theoretical models. *JOSA B*, 6(11):2023–2045, 1989.

[18] TL Gustavson, AP Chikkatur, AE Leanhardt, A Görlitz, Subhadeep Gupta, DE Pritchard, and Wolfgang Ketterle. Transport of bose-einstein condensates with optical tweezers. *Physical review letters*, 88(2):020401, 2001.

[19] Markus Greiner, Immanuel Bloch, Theodor W Hänsch, and Tilman Esslinger. Magnetic transport of trapped cold atoms over a large distance. *Physical Review A*, 63(3):031401, 2001.

[20] Christopher J Foot. *Atomic physics*. Oxford University Press, 2004.

[21] Wolfgang Petrich, Michael H Anderson, Jason R Ensher, and Eric A Cornell. Stable, tightly confining magnetic trap for evaporative cooling of neutral atoms. *Physical Review Letters*, 74(17):3352, 1995.

[22] F Schreck, G Ferrari, KL Corwin, Julien Cubizolles, L Khaykovich, M-O Mewes, and C Salomon. Sympathetic cooling of bosonic and fermionic lithium gases towards quantum degeneracy. *Physical Review A*, 64(1):011402, 2001.

[23] Harold J Metcalf and Peter Van der Straten. *Laser cooling and trapping*. Springer, 1999.

[24] Thad Walker, David Sesko, and Carl Wieman. Collective behavior of optically trapped neutral atoms. *Physical review letters*, 64(4):408, 1990.

[25] L Ricci, M Weidemüller, T Esslinger, A Hemmerich, C Zimmermann, V Vuletic, W König, and Th W Hänsch. A compact grating-stabilized diode laser system for atomic physics. *Optics Communications*, 117(5):541–549, 1995.

[26] TG Tiecke. Properties of potassium. *University of Amsterdam, The Netherlands, Thesis*, 2010.

[27] Heather J Lewandowski, DM Harber, Dwight L Whitaker, and EA Cornell. Simplified system for creating a bose–einstein condensate. *Journal of low temperature physics*, 132(5-6):309–367, 2003.

[28] Rudolf Grimm, Matthias Weidemüller, and Yurii B Ovchinnikov. Optical dipole traps for neutral atoms. *Advances in atomic, molecular, and optical physics*, 42:95–170, 2000.

[29] Daniel A Steck. Rubidium 87 d line data, 2001.

[30] F Dalfovo, L Pitaevskii, and S Stringari. The condensate wave function of a trapped atomic gas. *National Institute of Standards and Technology, Journal of Research*, 101(4):537–544, 1996.

[31] HMJM Boesten, CC Tsai, JR Gardner, DJ Heinzen, and BJ Verhaar. Observation of a shape resonance in the collision of two cold rb 87 atoms. *Physical Review A*, 55(1):636, 1997.